Universidad de Concepción
Departamento de Ingeniería Civil

Asociación Chilena de Sismología e
Ingeniería Antisísmica

N°A14-12 PSEUDO-DYNAMIC TESTING OF A LARGE SCALE COMPOSITE MRF UNDER EARTHQUAKE LOADING CONDITIONS.

Ricardo Herrera[1] , James M. Ricles, P.E.[2] , Richard Sause, P.E.[3]

1.- Departamento de Ingeniería Civil Universidad de Chile
Av. Blanco Encalada 2002, Piso 4, Santiago, Chile
e-mail: riherrer@ing.uchile.cl
2.- Lehigh University, Department of Civil and Environmental Engineering
117 ATLSS Drive, Bethlehem, PA 18015, USA
e-mail: jmr5@lehigh.edu
3.- Lehigh University, Department of Civil and Environmental Engineering
117 ATLSS Drive, Bethlehem, PA 18015, USA
e-mail: rs0c@lehigh.edu

SUMMARY

The seismic performance of composite moment frames with wide flange steel beams and concrete filled steel tubular columns (CFT-MRF) was experimentally studied. The test structure was a large scale model of a four-story prototype building with CFT-MRFs in the perimeter, designed according to current U.S. seismic provisions and recommendations from previous related research. The design of the prototype building was related to three seismic hazard levels, namely Frequent Occurrence (FOE), Design Basis (DBE), and Maximum Considered (MCE). The performance objectives of the prototype building were: only minor yielding under FOE level earthquakes; more extensive yielding and incipient local buckling on some members, but without strength degradation, under DBE level earthquakes; and collapse prevention under MCE level earthquakes. The test structure was subjected to simulated seismic solicitations, representative of the three seismic hazard levels, using the pseudo-dynamic hybrid testing methodology. The performance of the test structure was consistent with the prototype building expected performance, showing the applicability of this type of structures for seismic resistant design.

Keywords: Composite construction, Seismic performance, Concrete filled tubes, Pseudo-dynamic testing

1 INTRODUCTION

Composite steel-concrete construction makes use of the best characteristics of each material, combining the speed of construction, strength, long-span capability, and light weight of steel with the inherent stiffness, damping, and economy of concrete, resulting in an efficient structure. One particular form of composite member is a concrete filled steel tube (CFT). In a CFT, the steel tube replaces the formwork during construction, and confines the concrete infill during service, while the concrete infill restrains the local buckling of the steel tube, reducing the construction costs as well as the amount of transverse and longitudinal reinforcement required. In addition, the concrete infill enhances the fire resistance of the CFT column by acting as a heat sink (Shakir-Khalil 1988). Moment resisting frames (MRFs) composed of CFT columns combined with wide flange steel beams (CFT-MRF) are one form of composite construction. This system provides a lightweight and ductile frame with the added stiffness of composite columns to control lateral drift.

Previous research has investigated the behavior of the different elements that compose a CFT-MRF, including columns, beams, connections, and panel zones. All of these studies indicate that CFT members can be expected to behave satisfactorily when used as part of a lateral load resisting system designed to withstand seismic excitations. Due to the increasing interest in the use of this type of frame, design codes and specifications have been developed for CFT elements, as well as for buildings with CFT components. However, there is currently a lack of experimental and analytical data on the behavior of complete structural systems with CFT members, hence, an expected behavior is assumed in order to design the building, based on the knowledge of steel or reinforced concrete structural behavior.

Testing was conducted on one-story, one-bay CFT column frames in Japan (Kawaguchi *et al.* 1996). The ten specimens tested included column width-to-thickness (b/t) ratios of 21, 39, and 54, and levels of axial load on the columns of 15, 30, and 50 percent of N_0, where N_0 is defined as:

$$N_0 = F_y \cdot A_s + f'_c \cdot A_c \tag{1.1}$$

where F_y and A_s are the yield stress and area of the steel tube, and f'_c and A_c are the compressive strength and area of the concrete infill. The beam was welded to the columns with through-type diaphragms, which had holes to allow concrete placement, and was designed to remain elastic throughout the test. The specimens were subjected to a cyclic displacement history. This study concluded that the frames tested consistently showed better hysteretic characteristics than a similar steel frame. The local buckling at the base of the columns was the principal cause for strength degradation. The beam remained elastic and the panel zones suffered only minor yielding. More recently, pseudo-dynamic tests on a full-scale composite frame were performed in Taiwan (Chen *et al.* 2004). The frame was composed of a concentrically braced frame with buckling restrained braces in the central bay and moment connections between steel beams and CFT columns in the exterior bays. The test results showed that most of the demand was carried by the braced frame while the moment connections did not reach levels of deformation representative of those

sustained by moment connections in MRFs. Previous large-scale tests of multi-bay, multiple floor CFT-MRF structures are non-existent.

The evident need for a better understanding of CFT-MRFs motivated the development of an analytical and experimental program to study the seismic behavior of these systems. As part of this study, accurate models of components of CFT-MRFs and procedures for modeling CFT-MRF systems for nonlinear time-history analysis were obtained from the analytical investigations, which were then used to generate a test structure for the experimental studies. This paper presents the details of the experimental studies on a CFT-MRF test specimen as part of the U.S.-Japan Cooperative Research Program in Composite and Hybrid Structures. The objectives of these studies were to provide new experimental data on the response of CFT-MRFs to seismic loading, investigate the performance of these systems for different seismic hazard levels, and provide data to validate the models developed during the analytical investigations.

2 DEVELOPMENT OF THE TEST STRUCTURE

The test structure corresponded to a scaled model of a prototype building designed according to current U.S. specifications (International 2000, AISC 1999, ACI 2002) and recommendations from previous related research (Koester 2000, Peng *et al* 2001, Varma *et al.* 2001). The floor plan of the prototype building is shown in Fig. 2.1. The prototype building had five stories, four above ground and a basement level. The main lateral force resisting system consisted on four CFT-MRFs (two in each direction) located on the perimeter of the building, as shown in Fig. 2.1. The CFT columns were made of high-strength A500 Grade 80 square steel tubes (yield strength Fy = 552 MPa) filled with concrete with a compressive strength f'c of 55 MPa. The beams were A992 wide flange (WF) steel beams (Fy = 345 MPa). The moment connections between the beams and columns of the CFT-MRFs consisted on split tee connections, where the tee stem was fillet welded to the beam flanges and the tee flanges were post-tensioned to the column using high-strength threaded rods (see Fig. 2.2).

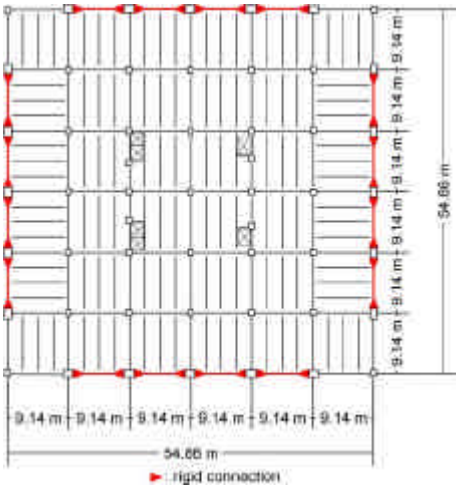

Figure 2.1: Prototype building floor plan

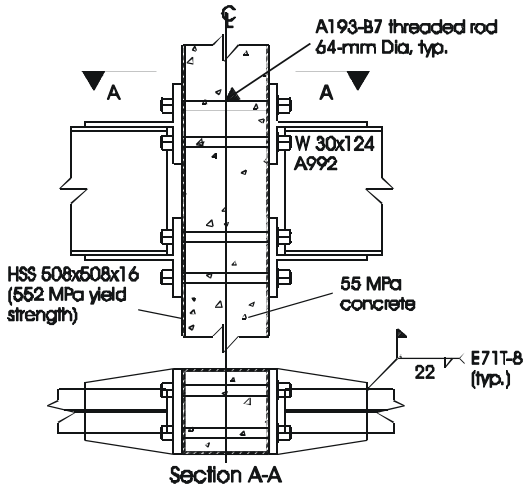

Figure 2.2: Typical moment connection

The performance of the building was related to three earthquake hazard levels, namely Maximum Considered (MCE, with a probability of exceedance of 2% in 50 years), Design Basis (DBE, equal to two-thirds of the MCE and with a probability of exceedance of approximately 10% in 50 years), and Frequent Occurrence (FOE, with a probability of exceedance of 50% in 50 years). The design objectives were expressed in terms of an expected performance of the building for each seismic hazard level: only minor yielding and concrete cracking occurring for FOE level earthquakes; more extensive yielding and incipient local buckling of the steel in beams and CFT columns, as well as cracking and incipient crushing of the concrete, but with no strength degradation for DBE level earthquakes; and collapse prevention for MCE level earthquakes.

A model of the prototype building was constructed using models developed previously for columns (Varma *et al* 2001), beams (Muhummud 2004), and connections (Peng *et al* 2001), as well as models developed as part of this study (panel zone model). The prototype building model accounted for nonlinearities associated with yielding and local buckling of steel, cracking and crushing of concrete, and geometric nonlinearities. The model was used to carry out inelastic analyses including time-history and static pushover analyses. The analysis results were then used to evaluate the performance of the prototype building and the ability of the provisions and design recommendations to provide a building design that achieved the design objectives. The details of the analytical studies are presented elsewhere (Herrera *et al.* 2003). Once the building design was considered satisfactory, a sub assemblage of the prototype building was selected as the test structure.

The test structure consisted of a three-fifths scale physical model of two bays of one of the CFT-MRFs on the perimeter of the prototype building, coupled with an analytical lean-on column representing the effect of the interior gravity frames of the prototype building tributary to the two bays of the CFT-MRF. The same materials selected for the prototype building were used for the test structure. A summary of the measured properties of the steel tubes, beams, and connection tees is shown in Table 2.1.

TABLE 2.1: AVERAGE MEASURED BEAM, TEE AND STEEL TUBE PROPERTIES

Section	Use in Test Structure	F_y (MPa) flange/web	F_{ys} (MPa) flange/web	F_u (MPa) flange/web
W18 X 143	Tee – G and 1st Floor	328.9/378.5	312.3/349.6	464.7/477.1
W18 X 130	Tee – 2nd Floor	343.4/389.6	321.3/366.1	496.4/496.4
W16 X 100	Tee – 3rd Floor	342.7/383.3	324.1/357.8	499.9/486.8
W18 X 71	Tee – 4th Floor	320.6/378.5	299.2/357.1	475.7/484.7
W18 X 46	Beam – 1st Floor	370.9/386.1	346.8/363.4	495.0/499.2
W16 X 40	Beam – 2nd Floor	333.0/392.3	311.0/365.4	457.1/488.1
W16 X 31	Beam – 3rd Floor	324.7/362.0	299.2/326.8	448.8/465.4
W12 X 22	Beam – 4th Floor	335.1/370.9	305.4/335.1	435.1/448.8
HSS 305x305x9.5	CFT columns*	559.2	523.3	646.7

Notes: F_y = Stress at 0.2% Offset Strain, F_{ys} = Static Yield Stress, F_u = Ultimate Strength

* 28-day concrete compressive strength f'_c = 67.6 MPa

The test structure beam and column sizes are shown in Fig. 2.3, where bay spacing and floor heights (top-of-steel dimensions) are also indicated. The scaled column, beam, and connection sizes were selected trying to maintain similitude on stiffness, strength, and slenderness parameters between the prototype building and the test structure.

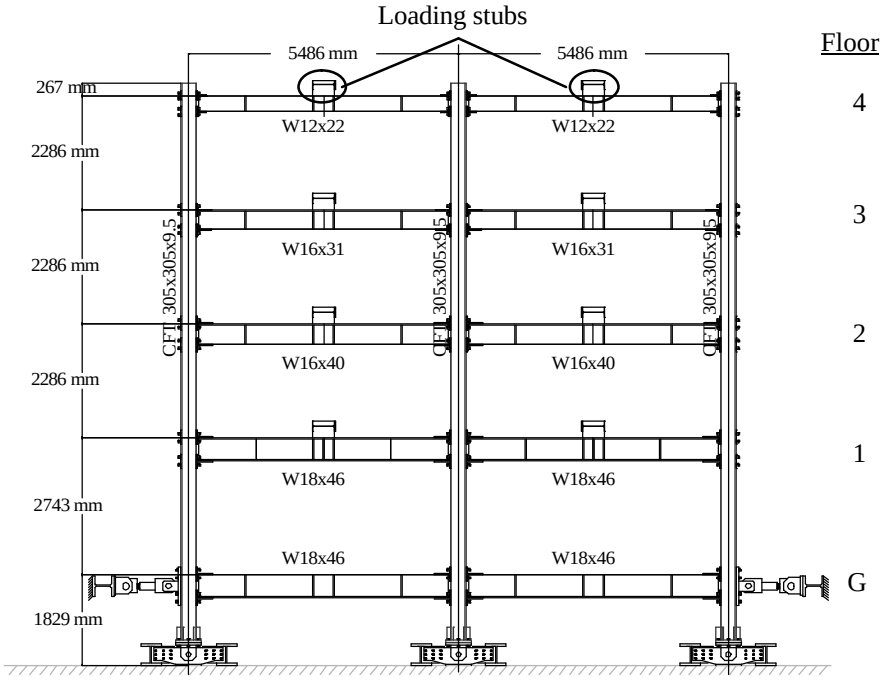

Figure 2.3: Test structure elevation

3 TESTING METHODOLOGY

Lateral displacements were imposed to the test structure by four hydraulic actuators (one at each floor level, excluding the ground) each connected to the test structure by loading beams attached at mid span to the test beams on each floor. These loading beams distributed the actuator load to both beams at every floor and served to simulate the restrain imposed by the floor slab on the axial deformation of the test beams.

The Pseudo-Dynamic (PSD) hybrid test method was used to test the test structure. The PSD method is a displacement-based control technique that requires solving the equation of motion of the test structure at each time step to determine the displacement target for the next step. The method assumes that the test structure can be represented accurately by a discrete-parameter model with a finite number of degrees of freedom (Mahin and Shing 1985), for which the equations of motion can be expressed as

$$M \cdot \ddot{u}(t) + C \cdot \dot{u}(t) + R(t) = P(t) \tag{3.1}$$

where

$$P(t) = -M \cdot ? \ddot{u}_g(t) \tag{3.2}$$

and M and C are the analytically defined mass and damping matrices of the structure, respectively, $\ddot{u}(t)$ and $\dot{u}(t)$ are the acceleration and velocity of the structure relative to the ground, respectively, $R(t)$ is the vector of restoring forces of the structure, $P(t)$ is the external force excitation, $?$ is the support motion influence vector (typically equal to a column vector of values of 1.0 for buildings), and $\ddot{u}_g(t)$ is the ground acceleration. Eq. (3.1) is solved using a numerical step-by-step integration method. For this study, the damping matrix C was a Rayleigh damping matrix calculated using the experimentally determined stiffness matrix K and the analytical mass matrix M, and assuming a damping ratio of 2% for the 1st and 3rd mode of the test structure.

Fig. 3.1 presents the general algorithm of the test methodology, which uses the explicit Newmark integration method (Newmark 1959) to solve the equations of motion of the test structure at each time step.

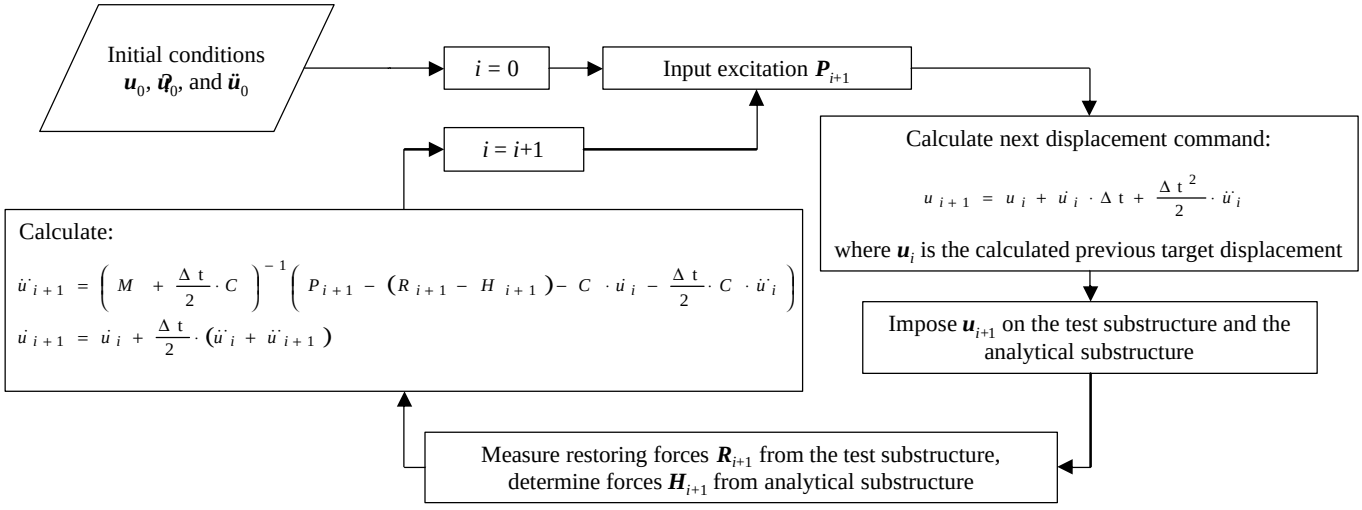

Figure 3.1: Pseudo-dynamic hybrid algorithm

The displacements u_{i+1} are imposed to the test structure and the restoring forces R_{i+1} and actual imposed displacements are measured; the restoring forces R_{i+1} are modified by the forces generated in the lean-on column (H_{i+1}) to account for the geometric effects of the gravity frames; the acceleration $\ddot{u}_{i+1}$ is calculated using the modified restoring forces and the external excitation P_{i+1}, and the velocity $\dot{u}_{i+1}$ is determined from the velocity on the previous step and the acceleration on the previous and current steps. The initial conditions of displacement (u_0) and velocity ($\dot{u}_0$) are generally equal to 0 in the case of earthquake excitation, and the acceleration ($\ddot{u}_0$) is determined from Eq. (3.1).

Being an explicit integration algorithm, the Newmark method is conditionally stable, i.e., the time step size must be kept below a maximum value for the solution to be numerically stable. For linear elastic structures, the time step must be smaller than T/π, where T is smallest period of the structure (Mahin and Shing 1985). There is also a restriction on the time step size based on the accuracy of the solution, which is generally more restrictive than the stability limit. No closed-form solution exists for the accuracy limit and in the case of non-linear structures, neither the stability nor the accuracy limits can be expressed in closed-form. A time step size of 0.0155 seconds (0.02 seconds at full scale) was found to be adequate through convergence studies conducted using a model of the test structure.

The main disadvantage of the PSD method is its sensitivity to error, either numerical or from displacement and restoring force feedback. To minimize the sources of error, and consequently improve the stability of the testing method, the calculated target displacements (instead of the actual displacements at the end of the time step) were used to calculate the next step target displacements, and small tolerances were set in order to ensure that the actual displacements were close enough to the target displacements. Moreover, the target displacement was approached asymptotically by successively applying a percentage of the difference between target and actual displacements.

Using the PSD hybrid test method, the test structure was subjected to several tests representative of the different seismic hazard levels. Only five tests, the most relevant, are presented here. The first four tests correspond to a FOE level, a DBE level, a MCE level, and a second DBE level intended to represent a large magnitude aftershock following the MCE level earthquake. The test structure was not repaired or modified in between these tests, except for a straightening process applied after the first DBE test to eliminate the residual drift on the structure induced by this test. Following the DBE aftershock, a few cycles of two MCE level earthquakes were applied quasi-statically to the test structure to obtain information about its failure mode. The history of displacements applied to the test structure during this last test had been previously determined by applying the earthquake records to the prototype building model, recording the displacement response of the prototype building, and scaling this response by the displacement scale factor (3/5). The list of tests is presented in Table 3.1. The fourth column in this table lists the factor by which the acceleration values were multiplied in order to represent the corresponding seismic hazard level. The time scale had to be multiplied by the square root of the scale factor to maintain dimensional similitude between the prototype building and the test structure.

TABLE 3.1 TEST MATRIX

Test Level	Record	Station	Scale Factor	Test Method
FOE	1979 Imperial Valley	Array 06	0.400	Pseudo-dynamic
DBE	1994 Northridge	Canoga Park	1.275	Pseudo-dynamic
MCE	1994 Northridge	Canoga Park	1.912	Pseudo-dynamic
DBE-A	1994 Northridge	Canoga Park	1.275	Pseudo-dynamic
MCEQcycl	1995 Kobe 1978 Miyagi-ken Oki	JMA Ofuna	0.777 0.810	Quasi-static

4 TEST STRUCTURE RESPONSE

4.1 FOE test

The displacement history applied to the test structure is shown in Fig. 4.1, where the time corresponds to the scaled time. The maximum displacement at the roof was 55 mm. corresponding to 0.6% of the total height of the building, measured from the ground to the top floor.

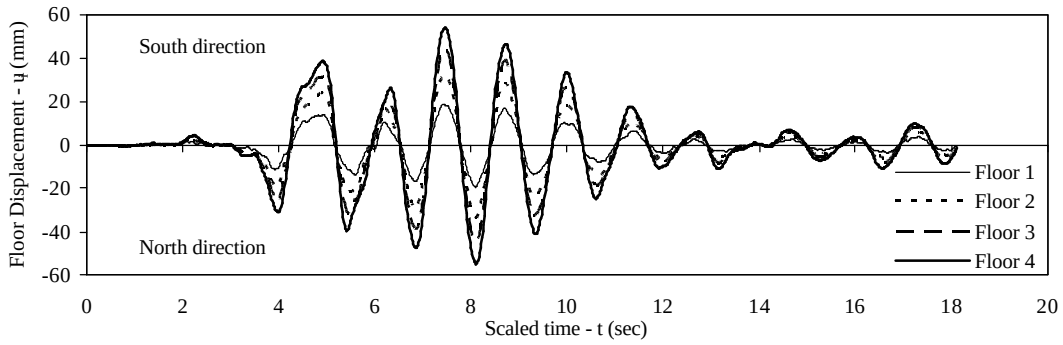

Figure 4.1: Displacement history applied during the FOE test

The test structure story drift-story shear response was primarily linear elastic as illustrated for the 1st story in Fig. 4.2. Approximately uniform values of maximum story drift ratio (defined as the story drift divided by the story height) were observed at all stories with values of 0.7%, 0.5%, 0.4%, and 0.4% at the 1st, 2nd, 3rd, and 4th story, respectively. For this level of drift almost no inelastic deformations were observed in the test structure with minor yielding only near the ends of the connections, on the beam flanges, as shown in Fig 4.3, and on the stem of the 4th floor bottom connection tees.

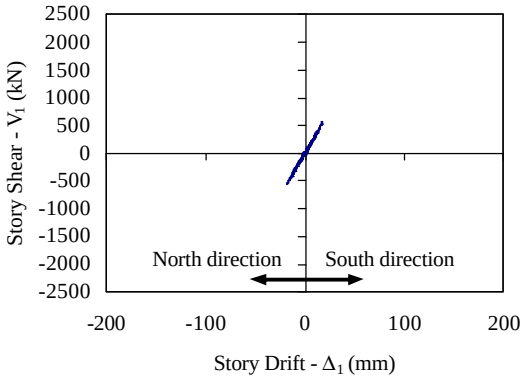

Figure 4.2: 1st story response

Figure 4.3: Beam yielding after FOE test

4.2 DBE test

The displacement history applied to the test structure during the DBE test is shown in Fig. 4.4. The maximum displacement at the roof was 285 mm. corresponding to 3.0% of the total height of the building, measured from the ground to the top floor. This test imposed inelastic deformations on the structure, as evidenced by the residual floor displacements that can be seen at the end of the test in Fig. 4.4.

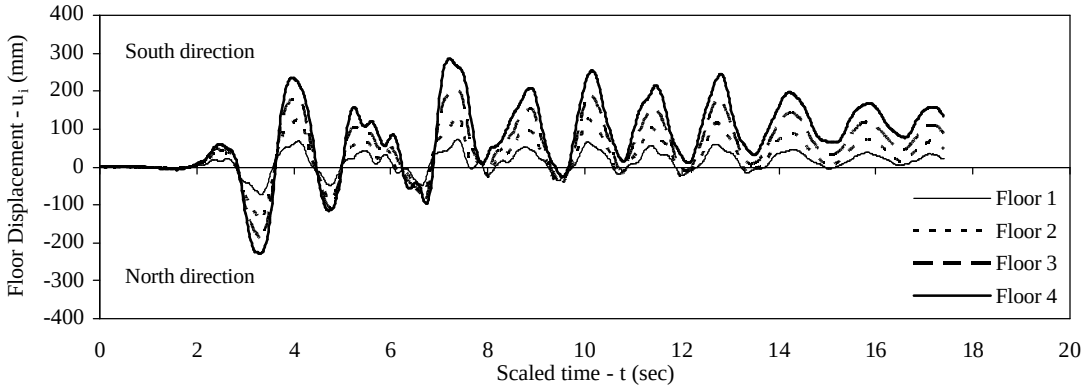

Figure 4.4: Displacement history applied during the DBE test

Inelastic response of the test structure was observed at all stories as illustrated for the 3rd story in Fig. 4.5. No degradation on the shear capacity could be observed at any story. The envelope story drift ratios are shown in Fig. 4.6, together with the maximum drift used for design, equal to 2.5% as prescribed by the IBC 2000 (International 2000). This limit was reached or exceeded at all floors with values of 2.5%, 2.9%, 3.9%, and 4.1% for the 1st, 2nd, 3rd, and 4th story, respectively. However, no significant strength degradation could be observed either at the story or at the member level, as shown by Figs. 4.5 and 4.7, respectively.

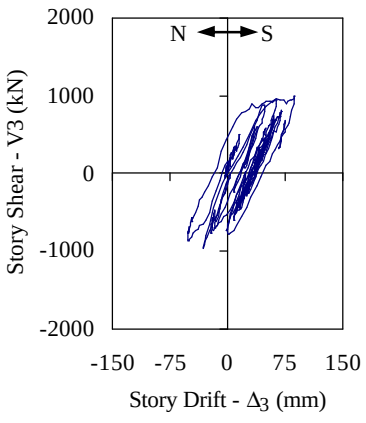

Figure 4.5: 3rd story response

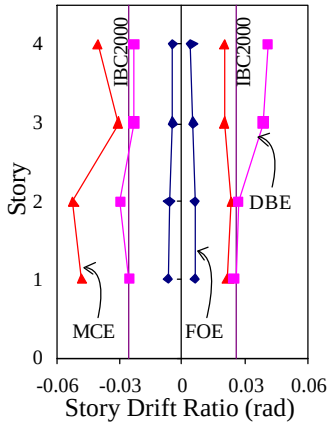

Figure 4.6: Story drift envelopes for FOE, DBE, and MCE tests

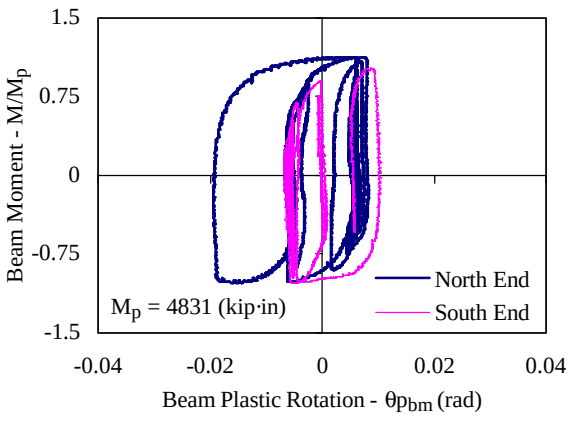

Figure 4.7: 1st floor north beam response

The exceedance of the drift limit is partly due to the effect of higher modes in the response of the test structure, and the inadequate estimate given by the code for the drift developed on a CFT-MRF under a DBE level earthquake.

Fig. 4.7 also shows that the beams had achieved their moment capacity and were developing plastic rotations, as it was expected for this level of seismic hazard according to the design philosophy. Yielding had extended from the flanges into the web at the beam ends and local buckling had developed at some of these locations, as shown in Figs. 4.8 and 4.9. When noticeable, the most pronounced local buckling was observed at the beam ends near the exterior connections (north end of the north beam and south end of the south beam), which were not prevented from shortening axially by the loading beams. The distribution of maximum total rotations measured at the base of the 1st story columns, beam ends, and connections is shown in Fig. 4.10 for the DBE test.

Figure 4.8: Beam yielding after DBE test

Figure 4.9: 3rd floor beam local buckling after DBE test

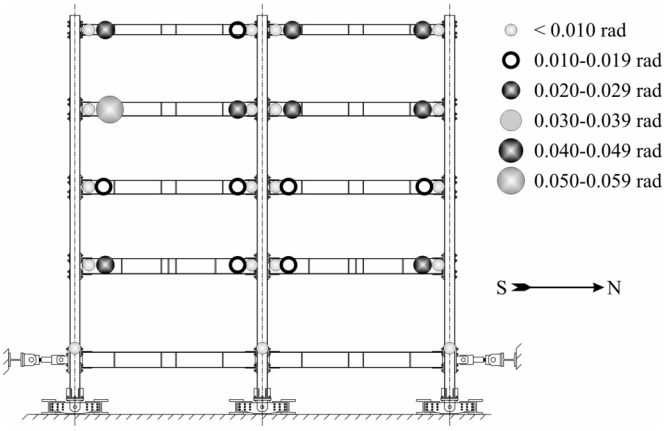

Figure 4.10: Maximum total rotation distribution, DBE

After the DBE test, the test structure was mechanically straightened y using the actuators at each floor level to eliminate the residual floor displacements before the application of the MCE level record.

4.3 MCE test

The displacement history applied to the test structure during the MCE test is shown in Fig. 4.11. The maximum displacement at the roof was 360 mm. corresponding to 3.7% of the total height of the building, measured from the ground to the top floor. The record produced inelastic deformations in the opposite

direction of those resulting from the DBE test, as evidenced by the residual floor displacements at the end of the MCE test in Fig. 4.11.

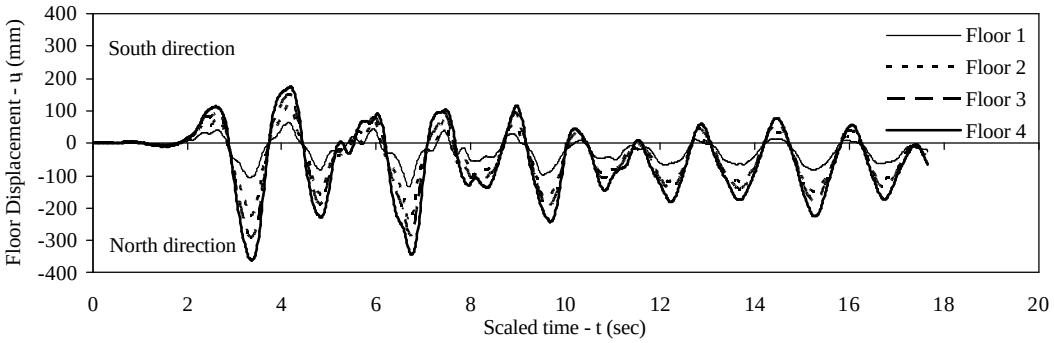

Figure 4.11: Displacement history applied during the MCE test

The maximum story drift ratios were 4.8%, 5.2%, 3.1%, and 4.0% at the 1st, 2nd, 3rd, and 4th story respectively, showing a larger demand on the lower stories with respect to the DBE test. At 6.63 seconds a loud noise was heard when a fracture developed at the bottom of the 1st story middle column, in line with the top rods of the ground connection tees. The drop in shear capacity at the 1st story upon fracture can be seen in Fig. 4.12. The fracture was not visible, but the necking of the material and change of color indicated its presence and location (see Fig. 4.13). The moment rotation response at the base of the 1st story middle CFT column is presented in Fig. 4.14.

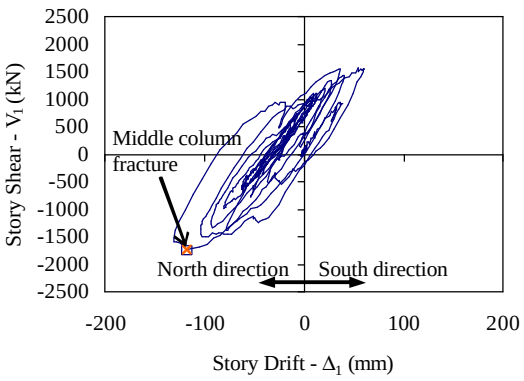

Figure 4.12: 1st story response

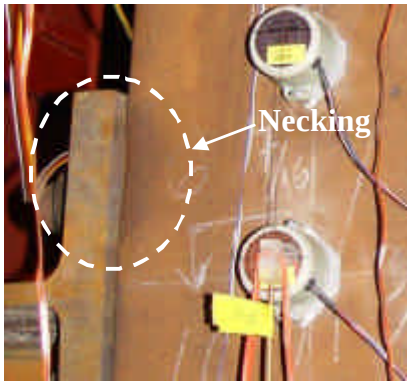

Figure 4.13: Fracture at the base of 1st story middle column

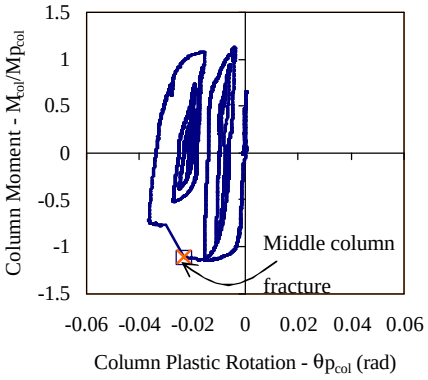

Figure 4.14: 1st floor middle column response

The observations at the end of the MCE test indicated that all beams had developed some degree of local buckling with the most pronounced buckling occurring in the exterior beam ends on every floor, as illustrated in Figs. 4.15(a) and (b). Yielding had extended to cover most of the beam section at all beam ends, indicating that the beams had reached their capacity and plastic hinges were developing at these locations. The distribution of maximum total rotations measured at the base of the 1st story columns, beam ends, and connections is shown in Fig. 4.16.

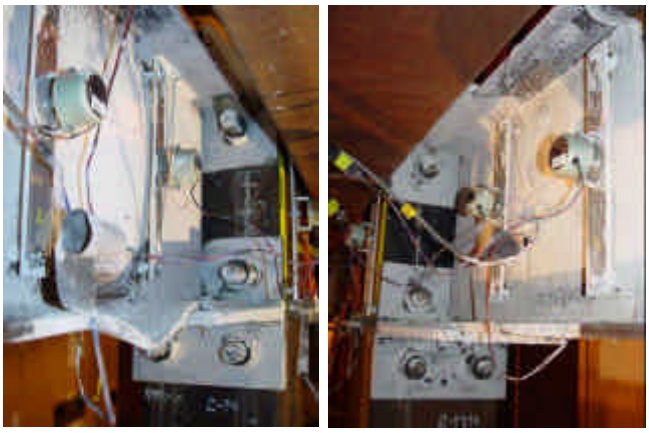

(a) North end (b) South end

Figure 4.15: 2nd floor north beam after MCE

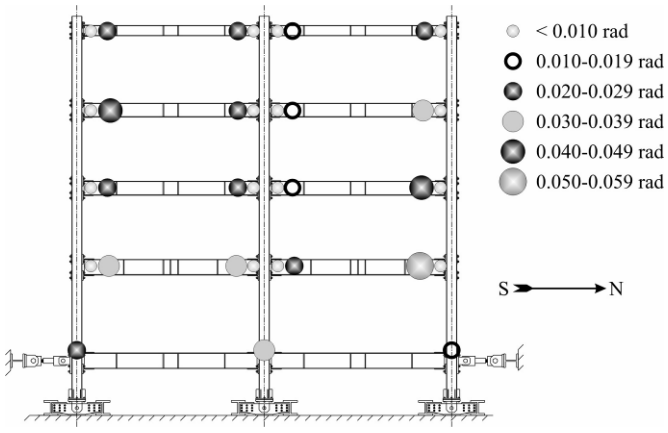

Figure 4.16: Maximum total rotation distribution, MCE

4.4 DBE-A test

The displacement history applied to the test structure during the DBE-A test is shown in Fig. 4.17.

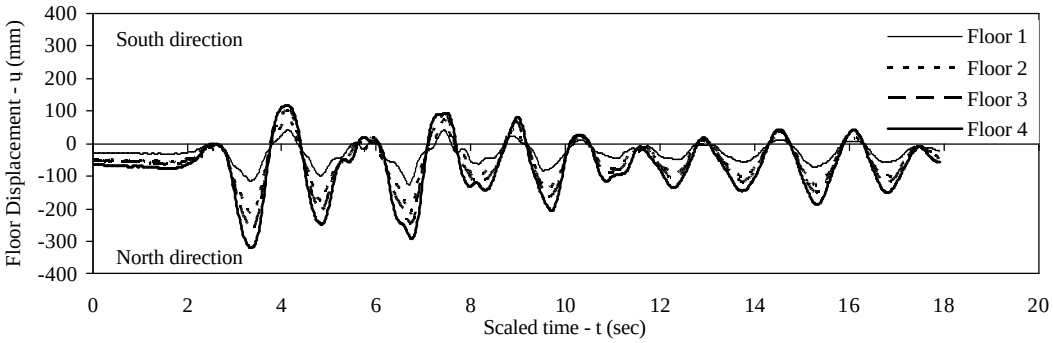

Figure 4.17: Displacement history applied during the DBE-A test

The maximum roof displacement was 319 mm. corresponding to 3.3% of the building height, measured from the ground to the top floor. The maximum story drifts did not exceed those observed during MCE, with maximum story drift ratios of 4.5%, 4.5%, 4.5%, and 4.5% at the 1st, 2nd, 3rd, and 4th stories, respectively. Fig. 4.18 shows the story shear-story drift response of the 1st story. Some pinching can be observed in this figure due to the propagation of the fracture on the middle column (shown in Fig. 4.19), as well as the generation of another fracture, located on the bottom flange of the north end of the 1st floor north beam (shown in Fig. 4.20).

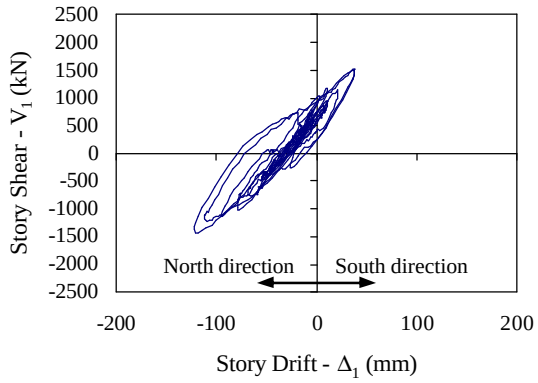

Figure 4.18: 1st story response

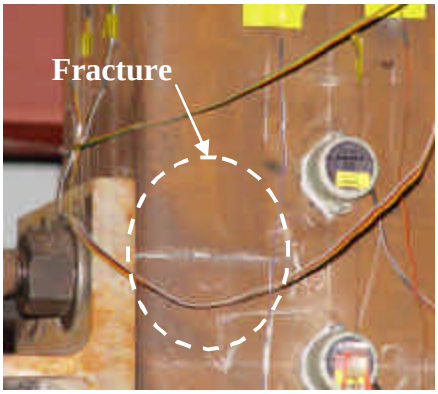

Figure 4.19: Fracture at the base of 1st story middle column

Figure 4.20: Fracture at the 1st floor north beam

Despite the two fractures, the test structure was able to sustain the DBE level aftershock without collapse.

4.5 MCEQcycl test

The displacement history applied to the test structure during the MCEQcycl test is shown in Fig. 4.21. The maximum roof displacement was 447 mm. corresponding to a 4.7% of the building height.

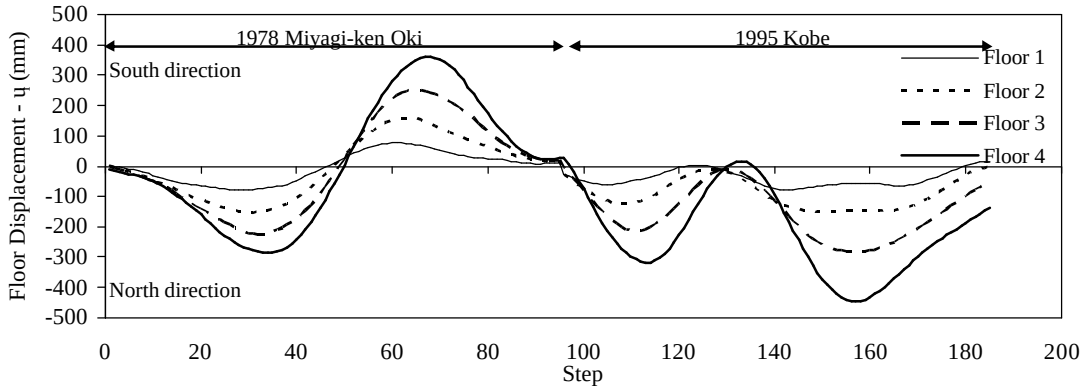

Figure 4.21: Displacement history applied during the MCEQcycl test

The displacements are plotted versus step because they correspond to only a few cycles of two MCE level records. The purpose of this test was to try to observe the dominant mechanisms of failure on the upper stories. Therefore, the floor displacement cycles were selected to impose more drift demand on these stories. A maximum story drift of 6.0% and 7.2% were imposed at the 3rd and 4th stories, respectively, both to the north. As a result of the large drift imposed on the 4th story, a sudden fracture occurred in the bottom flange at the south end of the south beam when the frame was being pushed to the maximum drift, as indicated in Fig. 4.22. The fracture extended across the whole flange as shown in Fig. 4.23.

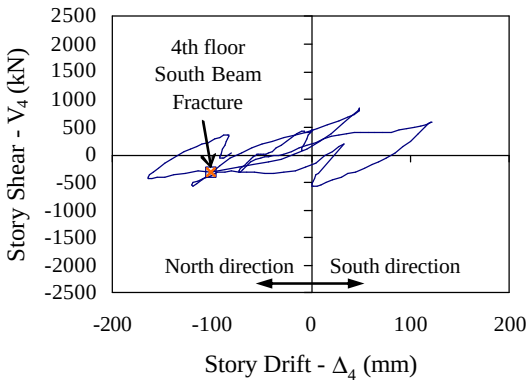

Figure 4.22: 4th story response

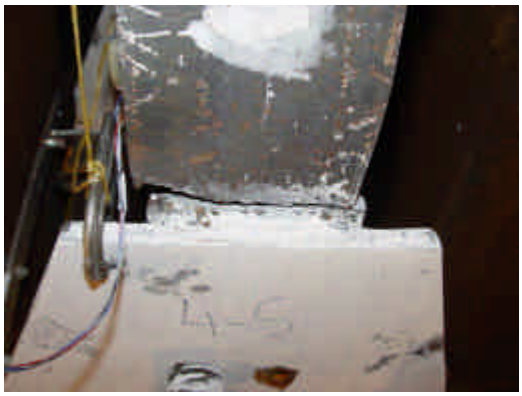

Figure 4.23: Fracture at the 4th floor south beam

In addition, the south column developed a fracture similar to that observed in the middle column. This fracture was the result of the increased demand on the north and south columns, due to the loss of capacity of the middle column caused by the propagation of the fracture generated during MCE. Upon unloading, the test structure was still standing, indicating the high degree of redundancy offered by this system.

5 CONCLUSIONS

The pseudo-dynamic hybrid test method successfully provided converged, stable displacement histories, representative of the corresponding seismic hazard levels.

Regarding the design objectives, the test structure suffered only minor yielding during the FOE level test, extensive yielding at all beam ends and incipient local buckling at a few beam ends during the DBE level test (but with no strength degradation), and extensive local buckling and yielding on all beam ends, as well as yielding and concrete crushing at the base of the 1st story columns, for the MCE level test. For this level, an unexpected fracture occurred at the base of one of the 1st story columns. However it did not hamper the stability of the structure, which was able to sustain a subsequent DBE level aftershock and a second partial MCE level displacement history. In summary, the structure response to the simulated earthquake excitations was consistent with the expected performance for all the hazard levels, indicating that composite MRFs with CFT columns can be effectively used to resist seismic loading conditions.

ACKNOWLEDGMENTS

The research reported herein was supported by the National Science Foundation (Dr. Shih-Chiu Liu cognizant program official), and by a grant from the Pennsylvania D.C.E.D. through the PITA program. The opinions expressed in this paper are those of the authors and do not necessarily reflect the views of the sponsors.

REFERENCES

Chen C.H., Hsiao B.C., Lai J.W., Lin M.L. ,Weng Y.T., and Tsai K. C. (2004). "Pseudo-dynamic Test of a Full-Scale CFT/BRB Frame: Part 2 - Construction and Testing", Proceedings 13WCEE, Vancouver, Canada, August 1-6.

Herrera R., Ricles J. M., and Sause R. (2003). "Analytical Studies of Steel MRFs with CFT Columns Under Earthquake Loading Conditions," Proceedings of STESSA 2003, Behaviour of Steel Structures in Seismic Areas, Naples, Italy, June 9-12.

International (2000). International Building Code, International Code Council (ICC), Falls Church, VA.

Kawaguchi J., Morino S., and Sugimoto T. (1996) "Elasto-Plastic Behavior of Concrete-Filled Steel Tubular Frames," Composite Construction in Steel and Concrete: Proceedings of an Engineering Foundation Conference, Irsee, Germany, June 9-14.

Koester B. (2000). "Panel Zone Behavior of Moment Connections between Rectangular Concrete-Filled Steel Tubes and WF Beams," Ph.D. Dissertation. Department of Civil and Environmental Engineering, University of Texas, Austin, TX.

Mahin S.A. and Shing P.B. (1985). "Pseudodynamic Method for Seismic Performance Testing", *ASCE, Journal of Structural Engineering* **111: 7**, pp. 1482-1503.

Muhummud, T. (2004). "Seismic Design and Behavior of Composite Moment Resisting Frame Constructed of CFT Columns and WF Beams." Ph.D. Dissertation. Department of Civil and Environmental Engineering. Lehigh University, Bethlehem, PA.

Newmark N. M. (1959). "A Method of Computation for Structural Dynamics", *Journal of the Engineering Mechanics Division*, ASCE, **85**: EM3, pp. 67-94

Peng S.W., Ricles J.M., and Lu L.W. (2001). "Seismic Resistant Connections for Concrete Filled Column-to-WF Beam MRFs," ATLSS Engineering Research Center, Report No. 01-08. Lehigh University, Bethlehem, PA.

Shakir-Khalil H. (1988). "Steel-Concrete Composite Columns-I" in Steel-Concrete Composite Structures. Stability and Strength. R. Narayanan, Editor. Elsevier Applied Science, London, UK.

Varma A., Ricles J.M., Sause R., and Lu L.W. (2001). "Seismic Behavior, Analysis, and Design of High-Strength Square Concrete Filled Steel Tube (CFT) Columns." ATLSS Engineering Research Center, Report No. 01-01. Lehigh University, Bethlehem, PA.